Chaotic Modeling and Simulation (CMSIM) 2: 265–272, 2013

Observation of Chaotic behaviour in the CCJJ+DC model of Coupled Josephson Junctions

André E Botha[1] and Yu. M. Shukrinov[2]

[1] Department of Physics, University of South Africa, P.O. Box 392, Pretoria 0003, South Africa
(E-mail: bothaae@unisa.ac.za)
[2] Bogoliubov Laboratory of Theoretical Physics, Joint Institute for Nuclear Research, Dubna, Moscow Region, 141980, Russia
(E-mail: shukrinv@theo.jinr.ru)

Abstract. Erratic behaviour in the simulated current-voltage characteristics of coupled intrinsic Josephson junctions, for certain ranges of the parameters, are observed and are shown to be chaotic in origin. In order to demonstrate the chaotic origin of the erratic behaviour, the Lyapunov exponents for the system are calculated. System trajectories and their Poincaré maps are used to confirm the chaotic signature obtained from the Lyapunov spectrum in certain ranges of the bias current, below the break point current.
Keywords: Chaos; Hyperchaos; CCJJ+DC model; Intrinsic Josephson Junctions.

1 Introduction

Systems of coupled intrinsic Josephson junctions (IJJs) are prospective candidates for the development of superconducting electronic devices [1]. Questions about their dynamics are, for a variety of reasons, of great technological importance [2]. For example, systems of junctions can produce much greater power output that a single junction and they also provide a model which may help to elucidate the physics of high temperature superconductors (HTSC) [3,4]. The intrinsic Josephson effect (IJE) [5], i.e. tunneling of Cooper pairs between superconducting layers inside of strongly anisotropic layered HTSC, provides a further motivation for considering HTSC as stacks of coupled Josephson junctions. The IJE also plays an important role in determining the current voltage characteristics (CVC) of tunneling structures based on HTSC and the properties of the vortex structures in these materials.

Although there has been a recent report on the hyperchaotic behaviour of an array of two resistive-capacitive-inductive-shunted Josephson junctions [6], the so-called RCLSJJ model [7], chaotic behaviour does not feature in

Received: 30 March 2012 / Accepted: 12 September 2012

ISSN 2241-0503

the literature on other closely-related phenomenological models; such as, the capacitively-coupled model (CCJJ) [8], the resistive-capacitive shunted model (RCSJJ) [5,9], or the CCJJ plus diffusion current (DC) model [10,11] of the present work. One possible reason for the comparatively late discovery of chaos in these systems may be that the (often subtle) chaotic features may have been masked by numerical instability and added noise in simulations.

This paper is organized as follows. In Section 2 we present the CCJJ+DC model and describe the numerical method used to calculate the Lyapunov exponents. In Section 3 we describe the observation of erratic behaviour in the CVC, which led to the discovery of chaos in the model. In section 4 we demonstrate that the erratic behaviour is chaotic in origin by looking as the Lyapunov exponents, system trajectories and Poincaré maps. In Section 5 we conclude that the erratic behaviour is chaotic in origin and that experimental investigations are required to ascertain whether this feature of the model is observable in real systems that satisfy the assumptions of the CCJJ+DC model. We also suggest that further work could be done on developing methods for controlling the observed chaos (hyperchaos) in this model.

2 Theory and simulation methods

2.1 The CCJJ+DC model

We solve the system of dynamical equations for the gauge-invariant phase differences $\varphi_\ell(\tau) = \theta_{\ell+1}(\tau) - \theta_\ell(\tau) - \frac{2e}{\hbar}\int_\ell^{\ell+1} dz A_z(z,\tau)$ between superconducting layers (S-layers), for stacks consisting of different numbers of IJJs, within the framework of the CCJJ+DC model [12,13]. In this model, θ_ℓ is the phase of the order parameter in the ℓth S-layer and A_z is the vector potential in the insulating barrier. For a system of N junctions the equations are,

$$\frac{d\varphi_\ell}{d\tau} = \sum_{\ell'=1}^{N} A_{\ell\ell'} V_{\ell'} \quad \text{and} \tag{1}$$

$$\frac{dV_\ell}{d\tau} = I - \sin\varphi_\ell - \beta \sum_{\ell'=1}^{N} A_{\ell\ell'} V_{\ell'} \ , \tag{2}$$

where $\ell = 1, 2, \ldots, N$ and the matrix A contains coupling parameters such as α. Note that A differs in form depending on whether periodic or non-periodic boundary conditions (BCs) are used [14]. The dissipation parameter β is related to the McCumber parameter β_c as $\beta = 1/\sqrt{\beta_c}$. For the purpose of numerical simulations we make use of a dimensionless time parameter $\tau = t\omega_p$, where $\omega_p = \sqrt{2eI_c/(\hbar C)}$ is the plasma frequency, I_c is the critical current and C is the capacitance. We measure the DC voltage on each junction V_ℓ in units of the characteristic voltage $V_c = \hbar\omega_p/(2e)$ and the bias current I in units of I_c. The critical currents in these (series) systems can typically range from 1 to $1000\,\mu$A, corresponding to voltages of $RI_c \sim 1\,$mV across individual junctions. Further details concerning this model can be found in Refs. [14,15]

2.2 Calculation of Lyapunov exponents

The Lyapunov exponents of a nonlinear dynamical system provide a quantitative measure of the degree of chaos inherent in the system, i.e. they quantify the sensitivity of the system to changes in initial conditions [16]. Usually one Lyapunov exponent is associated with each independent coordinate in the system. The numerical value of this exponent then characterizes the long term average exponential convergence (negative exponent) or divergence (positive exponent) of that coordinate with respect to some arbitrarily small initial separation.

Although the calculation of the Lyapunov exponents is in principle straight forward, in numerical calculations one has to guard against cumulative round-off errors which occur because of the exponential manner in which the small initial differences in coordinates may be amplified. Since real experimental data sets are typically small and noisy, it has taken a sustained effort to develop efficient algorithms for estimating the Lyapunov exponents associated with chaotic data sets [17–20]. In the preset simulations, since the system of Eqns. (1) and (2) are know in analytical form, we make use of the well-known algorithm by Wolf *et al.* [17]. Unlike some other methods, which only calculate the maximal Lyapunov exponent [21,22], the algorithm by Wolf *et al.* calculates the full spectrum of Lyapunov exponents and thus allows one to distinguish between chaotic attractors, which are characterised by only one positive exponent, and hyperchaotic attractors, which is characterised by more than one positive exponent.

In addition to Eqs. (1) and (2), the algorithm by Wolf *et al.* requires analytical expressions for the action of the system Jacobian $\mathbf{J}$ on an arbitrary column vector $\mathbf{x} = (\varphi_1,\varphi_2,\ldots,\varphi_N,V_1,V_2,\ldots,V_N)^T$ in the (φ, V) coordinate space. For the present system the action of $\mathbf{J}$ on $\mathbf{x}$ is given by

$$\mathbf{Jx} = \begin{pmatrix} A_{11}V_1 + A_{12}V_2 + \ldots + A_{1N}V_N \\ A_{21}V_1 + A_{22}V_2 + \ldots + A_{2N}V_N \\ \vdots \\ A_{N1}V_1 + A_{N2}V_2 + \ldots + A_{NN}V_N \\ -\varphi_1\cos\varphi_1 - \beta A_{11}V_1 - \beta A_{12}V_2 - \ldots - \beta A_{1N}V_N \\ -\varphi_2\cos\varphi_2 - \beta A_{21}V_1 - \beta A_{22}V_2 - \ldots - \beta A_{2N}V_N \\ \vdots \\ -\varphi_N\cos\varphi_N - \beta A_{N1}V_1 - \beta A_{N2}V_2 - \ldots - \beta A_{NN}V_N \end{pmatrix} \tag{3}$$

To calculate the Lyapunov exponents for a particular current I, we typically used 30000 dimensionless time steps, with a step size of $\Delta\tau = 0.2$. In all our calculations the number of steps and step size were chosen so that the magnitude of the zero exponent always converged to a value which was at least two orders of magnitude smaller than the magnitude of the smallest non-zero exponent. A fifth-order Runge-Kutta integration scheme was used.

3 Observation of erratic behaviour in the CVC

Erratic behaviour was first observed in the simulated CVC for certain ranges of parameter values. Figure 1 presents the simulated outermost branches in the

CVC for a stack of nine IJJs. Here V is the sum of the time averaged voltages

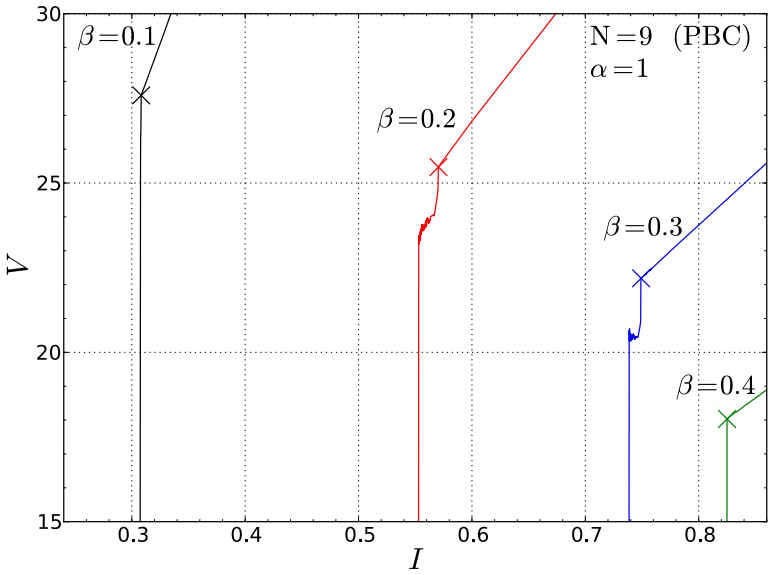

Fig. 1. Simulated outermost branches of the current voltage characteristics of an array with nine IJJ with $\alpha = 1$ and periodic boundary conditions (PBC). The curves for four different values of β are shown. The break point of each curve has been marked by a cross.

across each junction, i.e. $V = \langle V_1 \rangle + \langle V_2 \rangle + \ldots + \langle V_9 \rangle$, and I is bias current through the stack. As explained in Section 2.1, V and I are in units of V_c and I_c respectively. In Fig. 1 one can see the variation of the branch slope and the breakpoint (marked by a cross), for the four different values of dissipation parameter. As expected, the value of the break point current increases with increasing β; however, for $0.1 < \beta < 0.4$ the break point boarders on a so-called break point region (BPR). In Fig. 1 this region can be clearly seen to the left of the break points for the $\beta = 0.2$ and $\beta = 0.3$ curves. For these two values of β, erratic behaviour is observed to the left of each breakpoint. Initially this erratic behaviour was thought to be numerical in origin; however, as we will demonstrate in the next section, it is in fact chaotic.

4 Results and discussion

4.1 Demonstration of chaotic behaviour via Lyapunov exponents

Since we were unable to account for the observed erratic behaviour in terms of numerical instability, we decided to check whether or not the system is chaotic by calculating its Lyapunov exponents according to the method described in

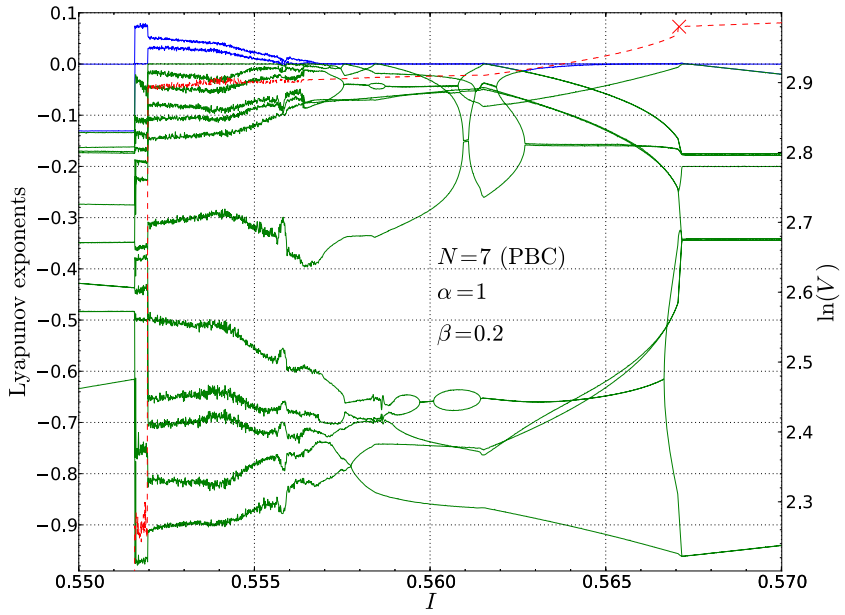

Fig. 2. Lyapunov exponents and CVC for a stack of seven IJJs with periodic boundary conditions.

Section 2.2. Typical results are shown in Fig. 2, for a stack of seven junctions, using the PBC. Here the left vertical axis is for the Lyapunov exponents $(\lambda_1, \ldots, \lambda_{14})$, while the right vertical axis is for $\ln(V)$ (red dashed curve). The largest two Lyapunov exponents, λ_1 and λ_2 (plotted in blue) both become positive exactly over the range of currents for which the erratic behaviour in V was observed, indicating that this system is hyperchaotic within the range $0.5520 < I < 0.5570$. In this range, as the current is decreased, λ_1 and λ_2 steadily increase, reaching their respective maxima of 0.052 and 0.031. At $I \approx 0.5520$ the system makes an abrupt transition to one of the inner branches of the CVC, over the range $0.5515 < I < 0.5520$. For the inner branch there is only one positive Lyapunov exponent ($\lambda_1 = 0.075$), which suggests that this transition may be associated with a change in the dynamics of the system, from hyperchaotic to chaotic. We have also performed other simulations at different parameter values and for N in the range 7-13, using both the PBC and NPBC. In all cases, for which erratic behaviour in the CVC was observed, we found either one or two positive Lyapunov exponent.

4.2 Comparison of system trajectories

To further verify that the observed behaviour is chaotic (hyperchaotic), we also looked at the system trajectory for a variety of different parameter values and initial conditions. Our observations are consistent with the values

obtained for the Lyapunov exponents. For example, Fig. 3 shows a projection onto the $\varphi_3 V_5$-plane of two different trajectories corresponding to a nine junction system ($N = 9$) with periodic boundary conditions and the parameters $\alpha = 1$ and $\beta = 0.2$. Both trajectories correspond to the outer branch

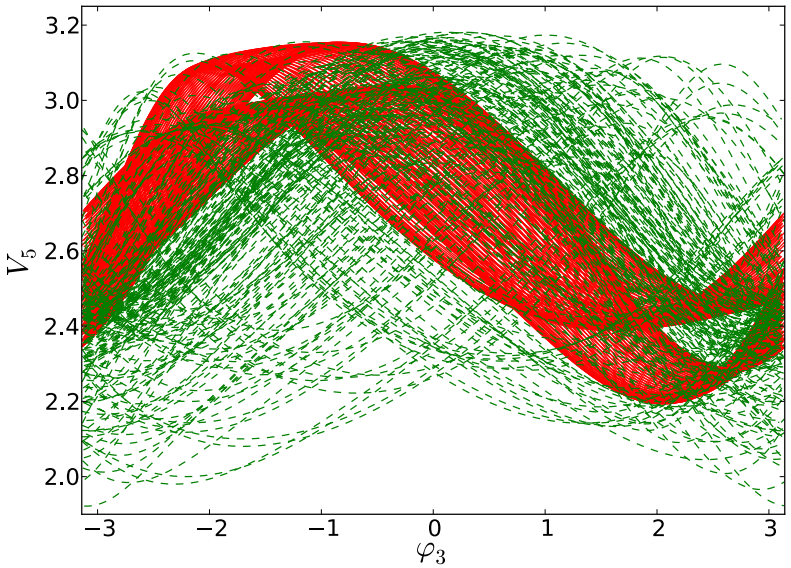

Fig. 3. A projection of two different system trajectories for a stack of nine IJJs with periodic boundary conditions. The solid red curve corresponds to a current above the break point value and is quasi-periodic, while the dashed green curve corresponds to a current below the break point, where the system is hyperchaotic.

of the CVC and have been integrated for 250 dimensionless time units. The solid red trajectory appears to be quasi-periodic, corresponding to $I = 0.5650$ and zero maximal Lyapunov exponent. The dashed green trajectory is hyperchaotic, corresponding to $I = 0.5575$, with the three largest exponents given by $\lambda_1 = 0.035$, $\lambda_2 = 0.022$ and $\lambda_3 = 0.00005$. In this figure the quasi-periodic nature of the non-chaotic trajectory (solid red curve) is clearly discernible from the hyperchaotic trajectory (dashed green curve).

4.3 Poincaré maps

To investigate further the differences between regular and chaotic regimes of the system, several Poincaré maps were constructed. Figure 4 shows a comparison of the maps for the trajectories described in Fig. 3. Here the intersection of the V_3V_9-projection of the trajectory with the plane $V_2 = 2.6$ is shown. Note the intersection is only from one side of the $V_2 = 2.6$ plane, i.e. the map was constructed by plotting the coordinates (V_3, V_9) for each intersection point, defined by a change in V_2 from $V_2 - 2.6 \leq 0$ to $0 \leq V_2 - 2.6$, over one

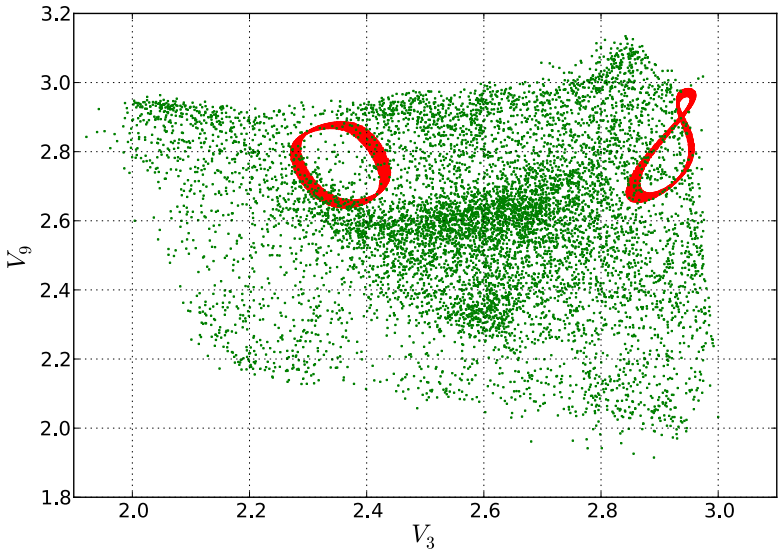

Fig. 4. Poincaré maps for the trajectories shown in Fig. 3. The intersection plane is given by $V_2 = 2.6$. The red pixels are for the intersection of the quasi-periodic trajectory while the green pixels are for the intersection of the hyperchaotic trajectory.

integration step. In order to obtain the large number of intersection points shown (between $8000 - 9000$ in each case) both trajectories were integrated for 20000 dimensionless time units, using a step size of $\Delta\tau = 0.025$. The quasi-periodic (hyperchaotic) behaviour of the red (green) trajectory is clearly visible, in agreement with Fig 3 and the calculated values of the Lyapunov exponents.

5 Conclusions

We have demonstrated that the observed erratic behaviour in our simulations of the CVC of coupled IJJs within the CCJJ+DC model is chaotic in origin. We have also shown that transitions can take place between hyperchaotic and chaotic dynamics, as the system jumps from the outermost CVC branch to inner branches. In this preliminary work we have not addressed many other important physical aspects; such as, the influence of the number of junctions, boundary conditions and charge correlations. A more detailed analysis of the chaos is currently in preparation [23].

In future work it would be interesting to establish whether or not the observed chaotic features in the present simulation are also experimentally observable in systems that satisfy the underlying assumptions of the CCJJ+DC model. Perhaps further work could also be done on controlling and exploiting (for technological use) the observed chaos (hyperchaos) in these systems.

References

1.R. Kleiner and P. Muller, Phys. Rev. B **94**, 1327 (1994).
2.L. Ozyuzer *et al.*, Science **318**, 1291 (2007).
3.K. Y. Tsang, R. E. Mirollo, S. H. Strogatz, and K. Wiesenfeld, Physica D **48**, 102 (1991).
4.S. H. Strogatz and R. E. Mirollo, Phys. Rev E **47**, 220 (1993).
5.W. Buckel and R. Kleiner, *Superconductivity: Fundamentals and Applications* (Wiley-VCH, Darmstadt, 2nd edition, 2004).
6.R. Ilmyong, F. Yu-Ling, Y. Zhi-Hai, and F. Jian, Chin. Phys. B **20**, 120504 (2011).
7.C. B. Whan and C. J. Lobb, Phys. Rev. E **53**, 405 (1996).
8.T. Koyama and M. Tachiki, Phys. Rev. B **54**, 16183 (1996).
9.C. B. Whan, C. J. Lobb, and M. G. Forrester, J. Appl. Phys. **77**, 382 (1995).
10.Y. M. Shukrinov, I. R. Rahmonov, and M. E. Demery, J. Phys.: Conf. Ser. **248**, 012042 (2010).
11.Y. M. Shukrinov and M. Hamdipour, Europhys. Lett. **92**, 37010 (2010).
12.M. Machida, T. Koyama, A. Tanaka, and M. Tachiki, Physica C **330**, 85 (2000).
13.Y. M. Shukrinov, F. Mahfouzi, and P. Seidel, Physica C **449**, 62 (2006).
14.Y. M. Shukrinov, F. Mahfouzi, and N. Pendersen, Phys. Rev. B **75**, 104508 (2007).
15.Y. M. Shukrinov and F. Mahfouzi, Phys. Rev. Lett. **98**, 157001 (2007).
16.J. C. Sprott, *Chaos and Time-Series Analysis* (Oxford University Press, London, 2003).
17.A. Wolf, J. B. Swift, H. L. Swinney, and J. A. Vastano, Physica D **16**, 285 (1985).
18.F. Sattin, Comput. Phy. Commun. **107**, 253 (1997).
19.T. Okushima, Phys. Rev. Lett. **91**, 254101 (2003).
20.Z.-M. Chen, K. Djidjeli, and W. G. Price, Applied Mathematics and Computation **174**, 982 (2006).
21.M. T. Rosenstein, J. J. Collins, and C. J. D. Luca, Physica D **65**, 117 (1993).
22.H. Kantz, Phys. Lett. A **185**, 77 (1994).
23.Y. M. Shukrinov, M. Hamdipour, M. R. Kolahchi, A. E. Botha, and M. Suzuki, Phys. Rev. B, in preparation.